symmetry

Article

Similarity Solution for Magnetogasdynamic Shock Waves in a Weakly Conducting Perfect Gas by Using the Lie Group Invariance Method

Gorakh Nath * and Kadam V S

Motilal Nehru National Institute of Technology Allahabad, Prayagraj 211 004, Uttar Pradesh, India; kadamvsrao@mnnit.ac.in

* Correspondence: gnath@mnnit.ac.in; Tel.: +91-8115-020-328

Abstract: Under axial and azimuthal magnetic inductions, the similarity solutions for a cylindrical shock wave in a weakly conducting ideal gas are determined using the Lie group invariance method. The axial and azimuthal magnetic inductions and density are presumed to vary in an ambient medium. This study determines the form of expression for axial and azimuthal magnetic inductions in the ambient medium. The ambient density is considered to be varying according to the power law of the shock radius. The weakly conducting medium causes inadequate magnetic freezing. We have numerically solved the system of ordinary differential equations that resulted from applying the Lie group invariance method to the system of partial differential equations. The impact of the variation in the ambient density exponent, the ratio of specific heats, magnetic Reynolds number, or the inverse square of axial and azimuthal Alfven Mach numbers on the shock strength and the flow variables behind the shock front is discussed. It is found that the shock strength decreases with an increase in the ratio of specific heats, magnetic Reynolds number, or the inverse square of axial and azimuthal Alfven Mach numbers.

Keywords: Lie group analysis; weakly conducting gases; axial and azimuthal magnetic inductions; cylindrical shock wave

Citation: Nath, G.; S, K.V. Similarity Solution for Magnetogasdynamic Shock Waves in a Weakly Conducting Perfect Gas by Using the Lie Group Invariance Method. *Symmetry* **2023**, *15*, 1640. https://doi.org/10.3390/sym15091640

Academic Editor: Christodoulos Sophocleous

Received: 28 July 2023
Revised: 22 August 2023
Accepted: 22 August 2023
Published: 25 August 2023

1. Introduction

Shock waves are powerful disturbances propagating through a medium, resulting in a sudden and significant change in flow variables such as pressure, temperature, density, etc. Shock wave generation can be achieved through different mechanisms, including explosive detonation, high-velocity projectiles, or focused energy sources like lasers. These methods induce a sudden release of energy, leading to the formation of shock waves that propagate outward from the source. Shock waves offer unique opportunities to investigate extreme conditions that are otherwise difficult to reproduce in a laboratory setting. They provide a means to explore phenomena such as high-temperature and high-pressure states, phase transitions, and chemical reactions under extreme conditions.

Understanding the fundamental physics of shock wave propagation under the influence of magnetic fields has implications in various fields. In astrophysics, the interaction of shock waves with magnetic fields is crucial for understanding the formation of stars, the dynamics of supernova remnants, and the acceleration of cosmic rays. In laboratory settings, strong magnetic fields in plasma physics and fusion reactions play a critical role in the confinement and compression of high-temperature plasmas (see [1–3]). The effects of magnetic fields on blast waves (see Sedov [4]) have been thoroughly addressed by Lerche [5,6] for both spherical and cylindrical geometries. By using the approach of Sedov (see Sedov [4]), Nath [7] has obtained self-similar solutions for strong cylindrical shock waves with isothermal flow conditions and investigated the effect of rotational parameters and the azimuthal magnetic field on the shock dynamics. Some of the important research on shock waves in magnetogasdynamic can be seen in (see [8,9]).

The behavior of shock waves in magnetic fields varies significantly between gases with high electrical conductivity, known as perfectly conducting gases, and those with low electrical conductivity, known as weakly conducting gases. In perfectly conducting gases, the magnetic field becomes closely intertwined with the fluid flow, resulting in magnetic freezing. This phenomenon occurs when the magnetic field lines attach to the fluid components, causing any changes in the compression or expansion of the fluid to impact the configuration of the magnetic field directly. Conversely, in weakly conducting gases with limited electrical conductivity, the interaction between shock waves, magnetic fields, and the gas itself is influenced by a combination of thermodynamic, hydrodynamic, and electromagnetic effects. Unlike perfectly conducting gases, weakly conducting gases do not exhibit complete magnetic freezing; instead, the magnetic field can partially penetrate the fluid, leading to a more intricate behavior of shock waves (see [10,11]).

The method of self-similarity (see Sedov [4]) was used by Vishwakarma and Patel [12] to describe cylindrical shock waves moving through a low-conducting gas medium while being influenced by the axial and azimuthal components of magnetic induction. By using the Chester–Chisnell–Whitham (CCW) approach, Vishwakarma and Srivastava [13] have investigated cylindrical detonation waves propagating in weakly ionized, strongly ionized, and non-ionized non-ideal gases under the influence of an azimuthal magnetic field. Under the influence of axial magnetic induction, Vishwakarma et al. [14] have investigated the similarity solutions in a weakly conducting dusty gas (a mixture of perfect gas and small solid particles).

Shock waves are frequently described using nonlinear partial differential equations (PDEs). To gain insight into the mathematical aspects and analyze these shock waves, we have employed the Lie group invariance method (LGIM). This method is known for its effectiveness and provides a structured approach to examining shock wave characteristics by converting the governing nonlinear PDEs into a set of ordinary differential equations (ODEs) using symmetries of differential equations (see [15–20]). Golovin [21] has discussed the bases of differential invariants for infinite-dimensional Lie groups. The possibilities of bases applications to construct differentially invariant solutions for the Navier–Stokes and gas dynamics equations are also discussed in [21]. Golovin [22] has examined the incompressible and stationary flows of an ideal plasma with constant total pressure by employing a curvilinear coordinate system in which streamlines and magnetic force lines collectively establish a set of coordinate surfaces, and the partial integral of the MHD equations are obtained and reformulated into a more convenient expression. The classes of solutions with constant total pressure in the case of non-stationary flows have been investigated by Golovin [23]. Dorodnitsyn and Kaptsov [24] have studied the one-dimensional shallow-water equations in Eulerian and Lagrangian coordinates. They have derived the relationship between symmetries and conservation laws in Lagrangian coordinates. Furthermore, the Lie group classification of the two-dimensional shallow-water equations with variable bottom topography in Lagrangian coordinates is discussed by Dorodnitsyn et al. [25]. Many mathematicians and physicists have used the Lie group analysis method to study differential equations that describe a wide range of physical phenomena and problems (see [26–28]).

As known to us, no one has used the Lie group invariance technique to investigate the similarity solution for a cylindrical shock wave propagating through a weakly conducting, ideal gas medium subjected to axial and azimuthal magnetic inductions. In this study, by utilizing the Lie group theoretical method, we have obtained the similarity solutions for shock waves propagating in a weakly conducting perfect gas under the influence of azimuthal and axial magnetic inductions. The effects of the adiabatic index, the ambient density variation exponent, magnetic Reynolds number, and the inverse square of azimuthal and axial Alfven Mach numbers on the shock strength and the flow variables behind the shock front are discussed. It is found that the shock waves decay with an increase in the value of the ratio of the specific heat. Furthermore, the parameter ratio of specific heats, magnetic Reynolds number, and the inverse square of axial and azimuthal Alfven Mach numbers have similar effects on the shock strength.

2. Governing Equations

In the presence of axial and azimuthal magnetic inductions, the fundamental equations describing the unsteady, cylindrically symmetric motion of a weakly conducting gas are (Taylor [29], Sakurai [11], Vishwakarma and Patel [12])

$$\frac{\partial \rho}{\partial t} + u\frac{\partial \rho}{\partial r} + \rho\frac{\partial u}{\partial r} + \frac{u\rho}{r} = 0, \tag{1}$$

$$\frac{\partial u}{\partial t} + u\frac{\partial u}{\partial r} + \frac{1}{\rho}\frac{\partial p}{\partial r} + \frac{1}{\rho}\sigma u(B_{z_0}^2 + B_{\theta_0}^2) = 0, \tag{2}$$

$$\frac{\partial p}{\partial t} + u\frac{\partial p}{\partial r} - a^2\left(\frac{\partial \rho}{\partial t} + u\frac{\partial \rho}{\partial r}\right) - (\gamma - 1)\sigma u^2(B_{z_0}^2 + B_{\theta_0}^2) = 0, \tag{3}$$

$$\frac{\partial B_z}{\partial r} - \mu\sigma u B_{z_0} = 0, \tag{4}$$

$$\frac{1}{r}\frac{\partial}{\partial r}(rB_\theta) - \mu\sigma u B_{\theta_0} = 0. \tag{5}$$

where σ is the electrical conductivity, γ is the ratio of specific heats, μ is the magnetic permeability, and B_{θ_0} and B_{z_0} are the azimuthal and axial magnetic inductions in the medium ahead of the shock front, respectively. B_θ, B_z, p, u, and ρ are the azimuthal magnetic induction, axial magnetic induction, pressure, velocity, and density, respectively; t and r represent the time and space coordinates.

The internal energy per unit mass of the gas I_e and the speed of sound a in the gas are given by

$$a^2 = \frac{\gamma p}{\rho}, \quad I_e = \frac{p}{\rho(\gamma - 1)}. \tag{6}$$

The azimuthal and axial magnetic inductions immediately ahead of the shock front are functions of time t only and are given by

$$B_{z0} = f(t), \quad B_{\theta 0} = g(t). \tag{7}$$

The cylindrical shock wave is generated by an explosion along the axis of symmetry, and it travels through a weakly conducting gas subjected to azimuthal and axial magnetic inductions, i.e., B_{θ_0} and B_{z_0}. Across the shock front, the magnetic induction can be continuous, as σ is considered small. The shock jump conditions across a strong shock were obtained by (Sakurai [11], Vishwakarma and Srivastava [13], Vishawakarma et al. [14], Vishwakarma and Patel [12]),

$$u_1 = \frac{2}{\gamma + 1}D, \quad \rho_1 = \frac{\gamma + 1}{\gamma - 1}\rho_0, \quad p_1 = \frac{2}{\gamma + 1}\rho_0 D^2, \quad B_{z1} = B_{z0}, \quad B_{\theta 1} = B_{\theta 0}. \tag{8}$$

where D is the shock front's velocity, and 0 and 1 refer to the conditions immediately ahead and behind of the shock front, respectively. An azimuthal Alfven Mach number M_{a_θ}, axial Alfven Mach number M_{a_z}, magnetic Reynolds number R_m, and velocity of shock front are defined by

$$M_{a_\theta} = \left(\frac{\mu\rho_0 D^2}{B_{\theta_0}^2}\right)^{-1/2}, \quad M_{a_z} = \left(\frac{\mu\rho_0 D^2}{B_{z_0}^2}\right)^{-1/2}, \quad R_m = \mu\sigma R D, \quad D = \frac{dR}{dt}, \tag{9}$$

where R is the shock radius.

3. Similarity Analysis by Using Invariance Group

To develop the similarity solution, we take a one-parameter Lie group of infinitesimal transformations as

$$\begin{aligned}&t^* = t + \epsilon\psi(t,r,\rho,u,B_z,B_\theta,p),\ r^* = r + \epsilon\chi(t,r,\rho,u,B_z,B_\theta,p),\ \rho^* = \rho + \epsilon S(t,r,\rho,u,B_z,B_\theta,p),\\&u^* = u + \epsilon U(t,r,\rho,u,B_z,B_\theta,p),\ B_z^* = B_z + \epsilon F(t,r,\rho,u,B_z,B_\theta,p),\ B_\theta^* = B_\theta + \epsilon G(t,r,\rho,u,B_z,B_\theta,p),\\&p^* = p + \epsilon P(t,r,\rho,u,B_z,B_\theta,p),\end{aligned} \tag{10}$$

where the infinitesimal generators ψ, χ, S, U, F, G, and P are to be calculated so that the set of Equations (1) to (5), along with the jump conditions (8), are invariant with respect to the transformations in Equation (10) (see [15–20]). The quantity ϵ is so small that its square and higher powers can be neglected.

To carry out the analysis, we introduce more convenient notations. Let $x_1 = t$, $x_2 = r$, $v_1 = \rho$, $v_2 = u$, $v_3 = B_z$, $v_4 = B_\theta$, $v_5 = p$, and $p_i^\zeta = \frac{\partial v_\zeta}{\partial x_i}$, where $\zeta = 1,2,3,4,5$ and $i = 1,2$. By using these notations, the system of Equations (1) to (5) can be represented as

$$Z_k(x_i, v_\zeta, p_i^\zeta) = 0, \qquad k = (1,2,\ldots,5). \tag{11}$$

The above system is said to be constantly conformally invariant under the infinitesimal group of transformations in Equation (10), if there exist constants $\alpha_{ks^*}(k, s^* = 1,2,\ldots,5)$, such that

$$\Delta Z_k = \alpha_{ks^*} Z_{s^*}, \qquad (k = 1,2,\ldots,5), \tag{12}$$

where Δ is the Lie derivative in the direction of the extended vector field, and it is defined by

$$\Delta = \phi_i \frac{\partial}{\partial x_i} + \Omega_\zeta \frac{\partial}{\partial v_\zeta} + A_i^\zeta \frac{\partial}{\partial p_i^\zeta}, \tag{13}$$

where

$$A_i^\zeta = \frac{\partial \Omega_\zeta}{\partial x_i} + \frac{\partial \Omega_\zeta}{\partial v_\tau} p_i^\tau - \frac{\partial \phi_j}{\partial x_i} p_j^\zeta - \frac{\partial \phi_j}{\partial v_\tau} p_j^\zeta p_i^\tau, \tag{14}$$

where $i,j = 1,2$; $\zeta,\tau = 1,2,3,4,5$; and $\phi_1 = \psi$, $\phi_2 = \chi$, $\Omega_1 = S$, $\Omega_2 = U$, $\Omega_3 = F$, $\Omega_4 = G$, $\Omega_5 = P$.

The following determining equations can be derived from Equations (1) and (12):

$$\begin{aligned}&S_\rho - \psi_t - u\psi_r = \alpha_{11} - \tfrac{\gamma p}{\rho}\alpha_{15},\ S_u - \rho\psi_r = \alpha_{12},\ S_{Bz} = S_{B\theta} = 0,\ S_p = \alpha_{15},\ uS_{Bz} + \rho U_{Bz} = \alpha_{13},\\&uS_\rho + \rho U_\rho - \chi_t - u\chi_r + U = \alpha_{11}u - \tfrac{\gamma p u}{\rho}\alpha_{15},\ uS_u + \rho U_u - \rho\chi_r + S = \alpha_{11}\rho + \alpha_{12}u,\\&uS_{B\theta} + \rho U_{B\theta} = \alpha_{14},\ uS_p + \rho U_p = \tfrac{1}{\rho}\alpha_{12} + \alpha_{15}u,\\&S_t + uS_r + \rho U_r - \tfrac{\chi\rho u}{r^2} + \tfrac{u}{r}S + \tfrac{\rho}{r}U = \alpha_{11}\tfrac{\rho u}{r} + \alpha_{12}\tfrac{\sigma u}{r}(f^2(t) + g^2(t)) - \alpha_{13}\mu\sigma f(t)u\\&+\alpha_{14}(-\mu u\sigma g(t) + \tfrac{B_\theta}{r}) - \alpha_{15}(\gamma-1)\sigma u^2(f^2(t) + g^2(t)).\end{aligned} \tag{15}$$

The following determining equations can be derived from Equations (2) and (12):

$$\begin{aligned}&U_\rho = \alpha_{21} - \tfrac{\gamma p}{\rho}\alpha_{25},\ \ U_u - \psi_t - u\psi_r = \alpha_{22},\ U_{Bz} = 0,\ \ U_{B\theta} = 0,\ U_p - \tfrac{1}{\rho}\psi_r = \alpha_{25},\\&uU_\rho + \tfrac{1}{\rho}P_\rho = \alpha_{21}u - \tfrac{\gamma p u}{\rho}\alpha_{25},\ uU_u + \tfrac{1}{\rho}P_u - \chi_t - u\chi_r + U = \alpha_{21}\rho + \alpha_{22}u,\ uU_{Bz} + \tfrac{1}{\rho}P_{Bz} = \alpha_{23},\\&uU_{B\theta} + \tfrac{1}{\rho}P_{B\theta} = \alpha_{24},\ uU_p + \tfrac{1}{\rho}P_p - \tfrac{1}{\rho}\chi_r - \tfrac{1}{\rho^2}S = \alpha_{22}\tfrac{1}{\rho} + \alpha_{25}u,\\&U_t + uU_r + \tfrac{2u\sigma\psi}{\rho}(g'(t)g(t) + f'(t)f(t)) - \tfrac{\sigma u S}{\rho^2}(g^2(t) + f^2(t)) + \tfrac{\sigma U}{\rho}(g^2(t) + f^2(t)) = \alpha_{21}\tfrac{1}{r}\rho u\\&+\alpha_{22}\tfrac{\sigma u}{\rho}(g^2(t) + f^2(t)) - \alpha_{23}\mu\sigma u f(t) + \alpha_{24}(-\mu\sigma u g(t) + \tfrac{1}{r}B_\theta) - \alpha_{25}(\gamma-1)\sigma u^2(f^2(t) + g^2(t)).\end{aligned} \tag{16}$$

The following determining equations can be derived from Equations (3) and (12):

$$\begin{aligned}&F_r - \psi\mu\sigma u f'(t) - \mu\sigma U f(t) = \alpha_{31}\tfrac{\rho u}{r} + \alpha_{32}\tfrac{\sigma u}{r}(f^2(t) + g^2(t)) + \alpha_{34}(-\mu\sigma u g(t) + \tfrac{1}{r}B_\theta)\\&-\alpha_{33}\mu\sigma u f(t) - \alpha_{35}(\gamma-1)\sigma u^2(f^2(t) + g^2(t)), \alpha_{31} = \alpha_{32} = \alpha_{35} = 0,\ \psi_r = 0,\ , F_u = \alpha_{31}\rho + u\alpha_{32},\\&F_\rho = u\alpha_{31} - \tfrac{\gamma p u}{\rho}\alpha_{35}, F_{Bz} - \chi_r = \alpha_{33},\ F_{B\theta} = \alpha_{34},\ F_p = \alpha_{35}u + \tfrac{1}{\rho}\alpha_{32}.\end{aligned} \tag{17}$$

The following determining equations can be derived from Equations (4) and (12):

$$\begin{aligned}
&G_r - \mu\sigma u\psi g'(t) - \mu\sigma g(t)U + \tfrac{1}{r}G - \tfrac{\chi B_\theta}{r^2} = \alpha_{41}\tfrac{\rho u}{r} + \alpha_{42}\tfrac{\sigma u}{r}(f^2(t)+g^2(t)) - \alpha_{43}\mu\sigma u f(t)\\
&+\alpha_{44}(-\mu\sigma u g(t) + \tfrac{1}{r}B_\theta) - \alpha_{45}(\gamma-1)\sigma u^2(f^2(t)+g^2(t)),\ \alpha_{41}=\alpha_{42}=\alpha_{45}=0,\ \psi_r = 0,\\
&G_\rho = \alpha_{41}u - \tfrac{\gamma p u}{\rho}\alpha_{45},\ G_u = \alpha_{41}\rho + \alpha_{42}u,\ G_{B_z} = \alpha_{43},\ G_{B\theta} - \chi_r = \alpha_{44},\ G_p = \tfrac{1}{\rho}\alpha_{42} + u\alpha_{45}.
\end{aligned} \tag{18}$$

The following determining equations can be derived from Equations (5) and (12):

$$\begin{aligned}
&P_t + uP_r - \tfrac{\gamma p}{\rho}S_t - \tfrac{\gamma p u}{\rho}S_r - 2(\gamma-1)\sigma u U(f^2(t)+g^2(t)) - 2(\gamma-1)\sigma u^2\psi(g'(t)g(t)+f'(t)f(t))\\
&= \alpha_{51}\tfrac{\rho u}{r} + \alpha_{52}\tfrac{\sigma u}{r}(g^2(t)+f^2(t)) - \alpha_{53}\mu\sigma u f(t) + \alpha_{54}(-\mu\sigma u g(t) + \tfrac{1}{r}B_\theta)\\
&-\alpha_{55}(\gamma-1)\sigma u^2(f^2(t)+g^2(t)),\ P_\rho - \tfrac{\gamma p}{\rho}S_\rho + \tfrac{\gamma p}{\rho}\psi_t + \tfrac{\gamma p}{\rho}\psi_r + \tfrac{\gamma p}{\rho^2}S - \tfrac{\gamma}{\rho}P = \alpha_{51} - \tfrac{\gamma p}{\rho}\alpha_{55},\\
&P_u - \tfrac{\gamma p}{\rho}S_u = \alpha_{52},\ P_{B_z} - \tfrac{\gamma p}{\rho}S_{B_z} = 0,\ P_{B\theta} - \tfrac{\gamma p}{\rho}S_{B\theta} = 0,\ P_p - \tfrac{\gamma p}{\rho}S_p - \psi_t - u\psi_r = \alpha_{55},\\
&uP_u - \tfrac{\gamma p u}{\rho}S_u = \alpha_{51}\rho + \alpha_{52}u, uP_{B\theta} - \tfrac{\gamma p u}{\rho}S_{B\theta} = \alpha_{54},\ uP_p - \tfrac{\gamma p u}{\rho}S_p - \chi_t - u\chi_r + U = \alpha_{52}\tfrac{1}{\rho} + \alpha_{55}u,\\
&uP_\rho - \tfrac{\gamma p u}{\rho}S_\rho + \tfrac{\gamma p}{\rho}\chi_t + \tfrac{\gamma p u}{\rho}\chi_r + \tfrac{\gamma p u}{\rho^2}S - \tfrac{\gamma p}{\rho}U - \tfrac{\gamma u}{\rho}P = \alpha_{51}u - \tfrac{\gamma p u}{\rho}\alpha_{55},\ uP_{B_z} - \tfrac{\gamma p u}{\rho}S_{B_z} = \alpha_{53}.
\end{aligned} \tag{19}$$

Together with Equations (15)–(19) mentioned above, the partial derivative of ψ and χ with respect to ρ, u, B_z, B_θ, and p also vanishes, i.e., we have the relation

$$\chi = \chi(r,t),\quad \psi = \psi(r,t). \tag{20}$$

Solving the above system of over-determining Equations (15)–(19), with the use of Equation (20), we obtain the infinitesimal generators as follows

$$\begin{aligned}
&\psi = at + c,\ \chi = (\alpha_{22}+2a)r,\ S = (\alpha_{11}+a)\rho\ U = (\alpha_{22}+a)u,\ F = (\alpha_{33}+\alpha_{22}+2a)B_z,\\
&G = (\alpha_{44}+\alpha_{22}+2a)B_\theta,\ P = (\alpha_{11}+2\alpha_{22}+3a)p,
\end{aligned} \tag{21}$$

where a, c, α_{11}, α_{22}, α_{33}, and α_{44} are constants and satisfy the relations

$$\begin{aligned}
&f(t) = e^{(\alpha_{33}-\alpha_{22}-a)\int\frac{dt}{at+c}},\quad g(t) = e^{(\alpha_{44}-\alpha_{22}-a)\int\frac{dt}{at+c}},\quad \text{and}\\
&2(at+c)(f'(t)f(t)+g'(t)g(t)) - \alpha_{11}(g^2(t)+f^2(t)) = 0.
\end{aligned} \tag{22}$$

4. Similarity Solution

The expression for the infinitesimal generators has arbitrary constants, the values of which lead to different cases of possible solutions.

Case I: Let $a \neq 0$, $c = 0$; then, from Equation (21), we have the infinitesimal generators as

$$\begin{aligned}
&\psi = at,\ \chi = (\alpha_{22}+2a)r,\ S = (\alpha_{11}+a)\rho\ U = (\alpha_{22}+a)u,\ F = (\alpha_{33}+\alpha_{22}+2a)B_z,\\
&G = (\alpha_{44}+\alpha_{22}+2a)B_\theta,\ P = (\alpha_{11}+2\alpha_{22}+3a)p.
\end{aligned} \tag{23}$$

The similarity variable and the similarity transformations are obtained by using the invariant surface condition. In this case, invariant surface conditions for u, ρ, B_z, B_θ, and p lead to

$$\psi u_t + \chi u_r = U,\ \psi\rho_t + \chi\rho_r = S,\ \psi B_{zt} + \chi B_{zr} = F,\ \psi B_{\theta t} + \chi B_{\theta r} = G,\ \psi p_t + \chi p_r = P. \tag{24}$$

Integrating Equation (24) with the use of Equation (23), we obtain the expression for the flow variables in the following form

$$u = \hat{U}(\eta)t^{\theta_1 - 1},\ \rho = \hat{S}(\eta)t^{\theta_2},\ B_z = \hat{F}(\eta)t^{\left(\frac{\alpha_{33}}{a}+\theta_1\right)},\ B_\theta = \hat{G}(\eta)t^{\left(\frac{\alpha_{44}}{a}+\theta_1\right)},\ p = \hat{P}(\eta)t^{(\theta_2+2(\theta_1-1))}, \tag{25}$$

where $\theta_1 = (\frac{\alpha_{22}}{a}+2)$, and $\theta_2 = (\frac{\alpha_{11}}{a}+1)$. The functions $\hat{S}$, $\hat{U}$, $\hat{F}$, $\hat{G}$, and $\hat{P}$ are totally dependent on the similarity variable η, calculated as

$$\eta = \frac{r}{At^{\theta_1}}, \tag{26}$$

where A is a constant with dimension. Furthermore, we have

$$R = At^{\theta_1}, \quad D = \frac{dR}{dt} = \frac{\theta_1 R}{t}. \tag{27}$$

From Equation (25), the values of $\hat{S}$, $\hat{U}$, $\hat{F}$, $\hat{G}$, and $\hat{P}$ at $\eta = 1$ are obtained as follows

$$\begin{aligned} &u\big|_{\eta=1} = \hat{U}(1)t^{\theta_1 - 1}, \; \rho\big|_{\eta=1} = \hat{S}(1)t^{\theta_2}, \; B_z\big|_{\eta=1} = \hat{F}(1)t^{\left(\frac{\alpha_{33}}{a}+\theta_1\right)}, \; B_\theta\big|_{\eta=1} = \hat{G}(1)t^{\left(\frac{\alpha_{44}}{a}+\theta_1\right)}, \\ &p\big|_{\eta=1} = \hat{P}(1)t^{(\theta_2+2(\theta_1-1))}. \end{aligned} \tag{28}$$

The conditions given by Equation (22) determine the expression for the variation in the initial azimuthal and axial magnetic inductions, i.e., B_{θ_0} and B_{z_0}, respectively, in the medium ahead of the shock front. Thus, the expressions for B_{θ_0} and B_{z_0} are obtained as

$$B_{z0} = f(t) = B_{z_k} t^{(\alpha_{33}/a)-\theta_1+1}, \quad B_{\theta 0} = g(t) = B_{\theta_k} t^{(\alpha_{44}/a)-\theta_1+1}, \tag{29}$$

where B_{z_k} and B_{θ_k} are reference constants. In the ambient medium, the flow-variable initial density ρ_0 is assumed to be varying according to

$$\rho_0 = \rho_k R^{\lambda_1}, \tag{30}$$

where ρ_k is the reference constant.

From Equations (22) and (29), we have

$$\begin{aligned} &2at\Big(\big(\tfrac{\alpha_{33}}{a} - \theta_1 + 1\big)B_{z_k}^2 t^{2((\alpha_{33}/a)-\theta_1+1)-1} + \big(\tfrac{\alpha_{44}}{a} - \theta_1 + 1\big)B_{\theta_k}^2 t^{2((\alpha_{44}/a)-\theta_1+1)-1}\Big) \\ &-\alpha_{11}\Big(B_{z_k}^2 t^{2((\alpha_{33}/a)-\theta_1+1)} + B_{z\theta_k}^2 t^{2((\alpha_{44}/a)-\theta_1+1)}\Big) = 0. \end{aligned} \tag{31}$$

From Equations (9), (27), (29), and (30), we obtain

$$\begin{aligned} M_{az}^2 &= \tfrac{\mu\rho_0 D^2}{B_{z0}^2} = \tfrac{\mu\rho_k A^{2+\lambda_1}\theta_1^2}{B_{z_k}^2} t^{\lambda_1\theta_1+2(\theta_1-1)-2((\alpha_{33}/a)-\theta_1+1)}, \\ M_{a\theta}^2 &= \tfrac{\mu\rho_0 D^2}{B_{\theta_0}^2} = \tfrac{\mu\rho_k A^{2+\lambda_1}\theta_1^2}{B_{\theta_k}^2} t^{\lambda_1\theta_1+2(\theta_1-1)-2((\alpha_{44}/a)-\theta_1+1)}. \end{aligned} \tag{32}$$

For the existence of the similarity solution, the axial and azimuthal Alfven Mach numbers must be constant; thus, we obtain

$$\lambda_1\theta_1 + 2(\theta_1 - 1) - 2((\alpha_{33}/a) - \theta_1 + 1) = 0, \; \lambda_1\theta_1 + 2(\theta_1 - 1) - 2((\alpha_{44}/a) - \theta_1 + 1) = 0. \tag{33}$$

From Equations (8), (28), (29), and (30), the values of the functions $\hat{S}$, $\hat{U}$, $\hat{F}$, $\hat{G}$, and $\hat{P}$ at $\eta = 1$ are determined as

$$\hat{S}(1) = \frac{(\gamma+1)}{(\gamma-1)}\rho_k A^{\lambda_1}, \; \hat{U}(1) = \frac{2}{(\gamma+1)}A\theta_1, \; \hat{F}(1) = B_{z_k}, \; \hat{G}(1) = B_{\theta_k}, \; \hat{P}(1) = \frac{2}{(\gamma-1)}\rho_k\theta_1^2 A^{2+\lambda_1}, \tag{34}$$

where $\lambda_1\theta_1 - \theta_2 = 0$, and $\theta_1 = 1/2$.

Equation (31), after using the values from Equations (33) and (25), becomes

$$2((\alpha_{33}/a) - \theta_1 + 1) - \theta_2 + 1 = 0. \tag{35}$$

By using Equations (26), (27), (29), (30), (33), and (35), we obtain the similarity transformations as

$$\rho = \rho_0\bar{S}(\eta), \quad u = D\bar{U}(\eta), \quad B_z = \sqrt{\mu\rho_0}D\bar{F}(\eta), \quad B_\theta = \sqrt{\mu\rho_0}D\bar{G}(\eta), \quad p = \rho_0 D^2\bar{P}(\eta), \tag{36}$$

where

$$\bar{U}(\eta) = \frac{\hat{U}(\eta)}{A\theta_1},\ \bar{S}(\eta) = \frac{\hat{S}(\eta)}{\rho_k A^{\lambda_1}},\ \bar{F}(\eta) = \frac{\hat{F}(\eta)}{\sqrt{\mu\rho_k}\theta_1 A^{\frac{\lambda_1}{2}+1}},\ \bar{G}(\eta) = \frac{\hat{G}(\eta)}{\sqrt{\mu\rho_k}\theta_1 A^{\frac{\lambda_1}{2}+1}},\ \bar{P}(\eta) = \frac{\hat{P}(\eta)}{\rho_k A^{\lambda_1+2}\theta_1{}^2},$$
$$\frac{\alpha_{33}}{a} - \frac{\lambda_1\theta_1}{2} + 1 = 0,\ \frac{\alpha_{44}}{a} - \frac{\lambda_1\theta_1}{2} + 1 = 0. \tag{37}$$

Using Equation (36) into the system of Equations (1) to (5), on suppressing the bar sign and solving for S', U', F', G', and P', we have

$$(U-\eta)S' + \lambda_1 S + SU' + \frac{SU}{\eta} = 0, \tag{38}$$

$$(U-\eta)U' + \left(\frac{\theta_1 - 1}{\theta_1}\right)U + \frac{P'}{S} + \frac{UR_m}{S}\left(M_{a_z}^{-2} + M_{a_\theta}^{-2}\right) = 0, \tag{39}$$

$$F' - \frac{R_m U}{M_{a_z}} = 0, \tag{40}$$

$$G' + \frac{G}{\eta} - \frac{R_m U}{M_{a_\theta}} = 0, \tag{41}$$

$$(U-\eta)P' + (\lambda_1 + \frac{2(\theta_1 - 1)}{\theta_1})P - \frac{\gamma P}{S}((U-\eta)S' + \lambda_1 S) - (\gamma - 1)R_m\left(M_{a_z}^{-2} + M_{a_\theta}^{-2}\right)U^2 = 0, \tag{42}$$

where $R_m = \sigma\mu RD$ is the magnetic Reynolds number. By using Equations (34) and (37), the shock jump conditions for S, U, F, G, and P at $\eta = 1$ can be written as (after suppressing the bar sign)

$$U(1) = \frac{2}{\gamma+1},\ \ S(1) = \frac{\gamma+1}{\gamma-1},\ \ F(1) = \frac{1}{M_{a_z}},\ \ G(1) = \frac{1}{M_{a_\theta}},\ \ P(1) = \frac{2}{\gamma+1}. \tag{43}$$

At the inner expanding surface (IES) of the flow field, the normal velocity of the fluid on the surface is equal to the velocity of the surface, which is the kinematic condition behind the shock front. Using Equation (36), we can determine this kinematic condition, which is

$$U(\eta_p) = \eta_p, \tag{44}$$

where η_p is the value of η at the inner expanding surface (IES). The flow variables ρ, u, B_z, B_θ, and p are normalized with their values at the shock front (i.e., at $\eta = 1$) as

$$\frac{\rho}{\rho_1} = \frac{S(\eta)}{S(1)},\ \frac{u}{u_1} = \frac{U(\eta)}{U(1)},\ \frac{B_z}{B_{z_1}} = \frac{F(\eta)}{F(1)},\ \frac{B_\theta}{B_{\theta_1}} = \frac{G(\eta)}{G(1)},\ \frac{p}{p_1} = \frac{P(\eta)}{P(1)}. \tag{45}$$

5. Results and Discussion

Through numerical integration of Equations (38)–(42) with the boundary conditions (43) and (44), using the fourth-order Runge–Kutta technique, we obtain the variation in the flow variables behind the shock front. For numerical integration, the physical parameters are taken as (see [13,14]) $\lambda_1 = -1.5, -1, 0, 1, 1.5$; $\gamma = 4/3, 5/3$; $R_m = 0.01, 0.1$; $M_{a_z}^{-2} = 0.01, 0.5$; and $M_{a_\theta}^{-2} = 0.01, 0.1$.

The location of the inner expanding surface η_p for different values of γ and λ_1 with $M_{a_z}^{-2} = 0.01$, $M_{a_\theta}^{-2} = 0.01$, and $R_m = 0.1$ in the power law case is shown in Table 1. Table 2 represents the location of the inner expanding surface (IES) η_p for $\gamma = 5/3$ and $\lambda_1 = -0.25$ at several values of $M_{a_z}^{-2}$, $M_{a_\theta}^{-2}$, and R_m. Figure 1 represents the variation in the flow variables behind the shock front for several values of γ and λ_1 when taking $M_{a_z}^{-2} = 0.01$, $M_{a_\theta}^{-2} = 0.01$, and $R_m = 0.1$. Figure 2 represents the variation in the flow variables behind the shock front for several values of $M_{a_z}^{-2}$, $M_{a_\theta}^{-2}$, and R_m when taking $\gamma = 5/3$ and $\lambda_1 = -0.25$.

Table 1. Position of inner expanding surface η_p at different values of γ and λ_1 when $M_{a_z}^{-2} = 0.01$, $M_{a_\theta}^{-2} = 0.01$, and $R_m = 0.1$ for power law shock path case.

γ	λ_1	η_p Inner Expanding Surface (IES)
4/3	−1.5	0.928305
4/3	−1.0	0.895738
4/3	0.0	0.000012
4/3	1.0	0.843549
4/3	1.5	0.889101
5/3	−1.5	0.923135
5/3	−1.0	0.893536
5/3	0.0	0.00001
5/3	1.0	0.754601
5/3	1.5	0.813806

Table 2. Position of inner expanding surface η_p at different values of R_m, $M_{a_z}^{-2}$, and $M_{a_\theta}^{-2}$ when $\gamma = 5/3$ and $\lambda_1 = -0.25$ for power law shock path case.

R_m	$M_{a_z}^{-2}$	$M_{a_\theta}^{-2}$	η_p Inner Expanding Surface (IES)
0.01	0.01	0.01	0.586147
0.01	0.01	0.50	0.584657
0.01	0.50	0.01	0.584657
0.01	0.50	0.50	0.583242
0.1	0.01	0.01	0.585625
0.1	0.01	0.50	0.571565
0.1	0.50	0.01	0.571565
0.1	0.50	0.50	0.558567

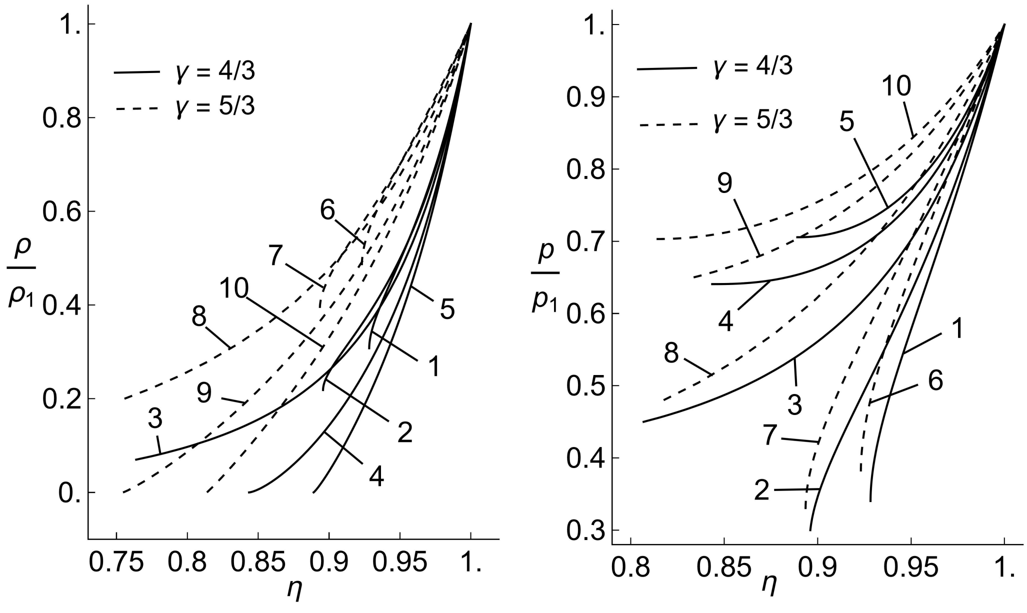

(**a**) (**b**)

Figure 1. *Cont.*

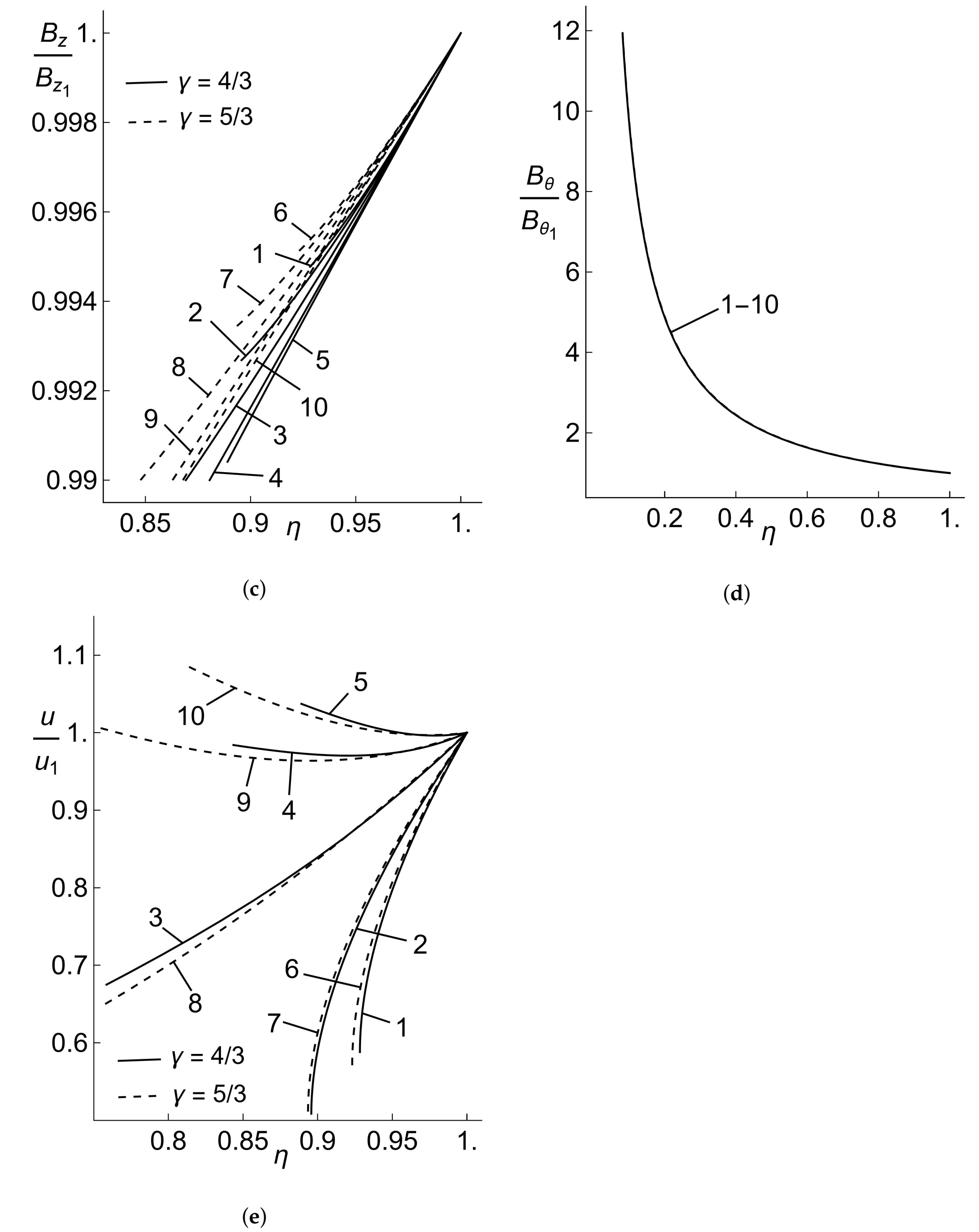

Figure 1. Distribution of the flow variables in the region behind the shock front for different values of γ and λ_1 when $R_m = 0.1$, $M_{a_z}^{-2} = 0.01$, and $M_{a_\theta}^{-2} = 0.01$ for power law shock path case: (**a**) density $\frac{\rho}{\rho_1}$, (**b**) pressure $\frac{p}{p_1}$, (**c**) axial magnetic induction $\frac{B_z}{B_{z_1}}$, (**d**) azimuthal magnetic induction $\frac{B_\theta}{B_{\theta_1}}$, (**e**) radial velocity $\frac{u}{u_1}$, 1. $\gamma = 4/3$, $\lambda_1 = -1.5$; 2. $\gamma = 4/3$, $\lambda_1 = -1$; 3. $\gamma = 4/3$, $\lambda_1 = 0$; 4. $\gamma = 4/3$, $\lambda_1 = 1$; 5. $\gamma = 4/3$, $\lambda_1 = 1.5$; 6. $\gamma = 5/3$, $\lambda_1 = -1.5$; 7. $\gamma = 5/3$, $\lambda_1 = -1$; 8. $\gamma = 5/3$, $\lambda_1 = 0$; 9. $\gamma = 5/3$, $\lambda_1 = 1$; 10. $\gamma = 5/3$, $\lambda_1 = 1.5$.

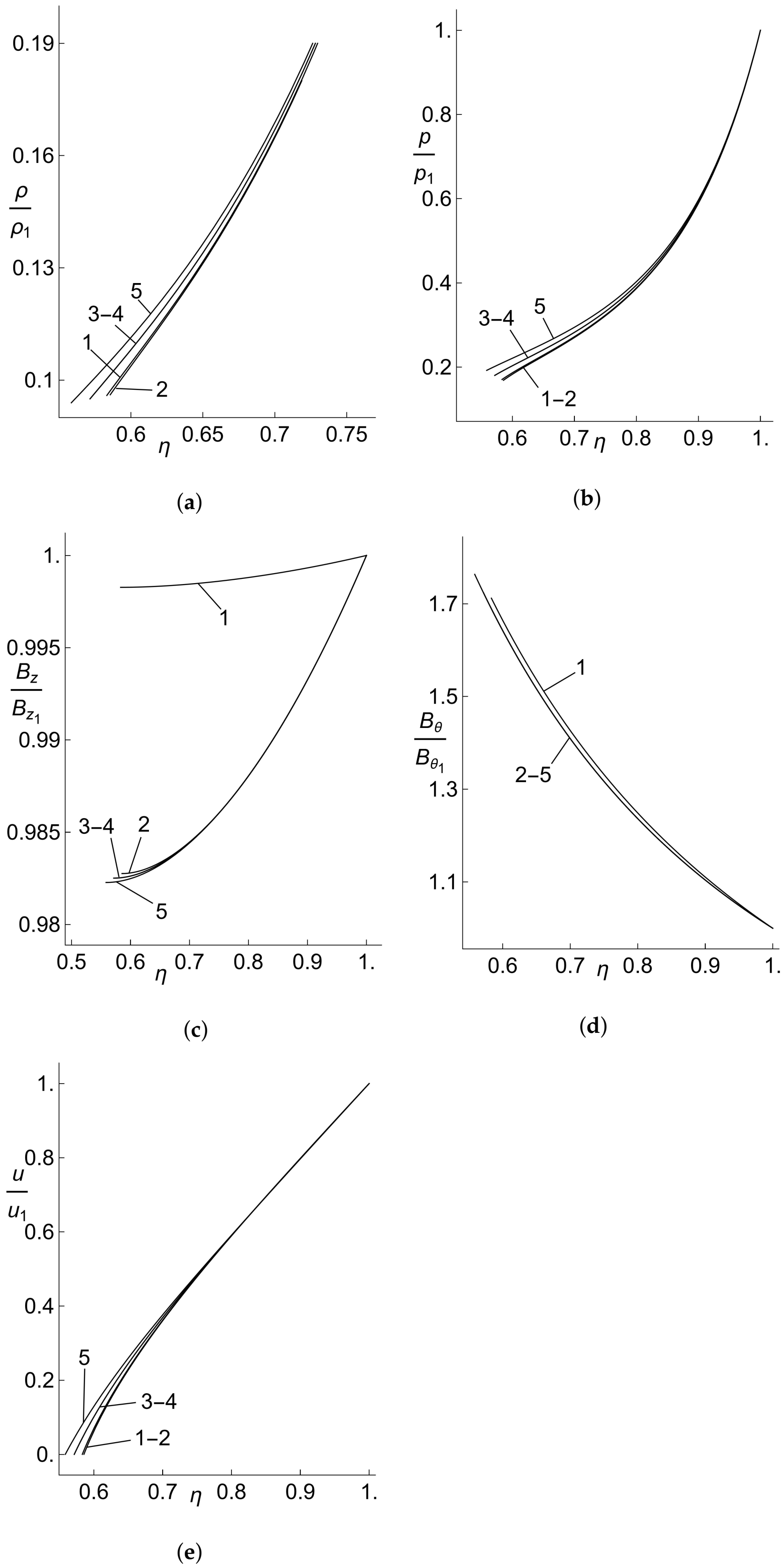

Figure 2. Distribution of the flow variables in the region behind the shock front for different values of R_m, $M_{a_z}^{-2}$, and $M_{a_\theta}^{-2}$ when $\gamma = 5/3$ and $\lambda_1 = -0.25$ for power law shock path case. (**a**) Density $\frac{\rho}{\rho_1}$, (**b**) pressure $\frac{p}{p_1}$, (**c**) axial magnetic induction $\frac{B_z}{B_{z_1}}$, (**d**) azimuthal magnetic induction $\frac{B_\theta}{B_{\theta_1}}$, (**e**) radial velocity $\frac{u}{u_1}$, 1. $R_m = 0.01$, $M_{a_z}^{-2} = 0.5$, $M_{a_\theta}^{-2} = 0.5$; 2. $R_m = 0.1$, $M_{a_z}^{-2} = 0.01$, $M_{a_\theta}^{-2} = 0.01$; 3. $R_m = 0.1$, $M_{a_z}^{-2} = 0.01$, $M_{a_\theta}^{-2} = 0.5$; 4. $R_m = 0.1$, $M_{a_z}^{-2} = 0.5$, $M_{a_\theta}^{-2} = 0.01$; 5. $R_m = 0.1$, $M_{a_z}^{-2} = 0.5$, $M_{a_\theta}^{-2} = 0.5$.

5.1. The Implications of a Rise in the Exponent of Ambient Density λ_1

For $\lambda_1 < 0$, η_p decreases, i.e., the distance between the shock front and the IES increases, which demonstrates that shock waves decay with an increase in λ_1, whereas for $\lambda_1 > 0$, η_p increases, i.e., the distance between the shock front and the IES decreases, which shows that shock becomes stronger with an increase in λ_1 (see Table 1). For $\lambda_1 < 0$ or $\lambda_1 > 0$, the pressure p/p_1 and fluid velocity u/u_1 increase, but the axial magnetic induction B_z/B_{z_1} decreases with an increase in λ_1 and the azimuthal magnetic induction B_θ/B_{θ_1} remains unchanged with λ_1 (see Figure 1b–e). The density ρ/ρ_1 increases near the IES, and it decreases near the shock front with λ_1 (see Figure 1a).

5.2. The Implications of a Rise in the Ratio of Specific Heats γ

The distance between the shock front and the IES increases with an increase in γ (see Table 1), demonstrating that the shock strength decreases when the adiabatic exponent increases. The flow variables ρ/ρ_1, p/p_1, and B_z/B_{z_1} increase, and B_θ/B_{θ_1} is almost unaffected with γ (see Figure 1a–d). For $\lambda_1 < 0$, the fluid velocity u/u_1 increases, and for $\lambda_1 > 0$ or $\lambda_1 = 0$, it decreases with an increase in γ (see Figure 1e).

5.3. The Implications of a Rise in the Magnetic Reynolds Number R_m

The value of IES η_p decreases with an increase in the magnetic Reynolds number R_m, demonstrating that the shock strength decreases with R_m (see Table 2). The density ρ/ρ_1, pressure p/p_1, and fluid velocity u/u_1 increase, but B_z/B_{z_1} and B_θ/B_{θ_1} decrease with an increase in R_m (see Figure 1a–e).

5.4. The Implications of a Rise in the Parameters $M_{a_z}^{-2}$ or $M_{a_\theta}^{-2}$

The value of IES η_p decreases with an increase in the value of $M_{a_z}^{-2}$ or $M_{a_\theta}^{-2}$, demonstrating that the shock strength decreases with $M_{a_z}^{-2}$ or $M_{a_\theta}^{-2}$ (see Table 2). The density ρ/ρ_1, pressure p/p_1, and fluid velocity u/u_1 increase, but the axial magnetic induction B_z/B_{z_1} decreases with an increase in $M_{a_z}^{-2}$ or $M_{a_\theta}^{-2}$, and almost no effect of these parameters on the azimuthal magnetic induction B_θ/B_{θ_1} is obtained (see Figure 1a–e).

6. Conclusions

In this work, we employ the Lie group invariance approach to explore the similarity solution for a cylindrical shock wave in a weakly conducting perfect gas subjected to azimuthal and axial magnetic inductions. Based on values of arbitrary constants in the expression for infinitesimal, we have determined the similarity solutions for the power law shock path. From Tables 1 and 2, and Figures 1 and 2, we have drawn the following conclusions:

1. The adiabatic exponent γ of the gas has decaying effects on the shock strength. The parameters γ, R_m, $M_{a_z}^{-2}$, or $M_{a_\theta}^{-2}$ have similar effects on the shock strength.
2. With an increase in magnetic Reynolds number R_m, pressure p/p_1, the density ρ/ρ_1 and fluid velocity u/u_1 increase, but the axial magnetic induction B_z/B_{z_1} decreases. The parameters $M_{a_z}^{-2}$, $M_{a_\theta}^{-2}$, and magnetic Reynolds number R_m have similar effects on ρ/ρ_1, p/p_1, u/u_1, and B_z/B_{z_1}.
3. The ambient density exponent λ_1 has a decaying impact on shock strength for $\lambda_1 < 0$, whereas shock strength increases for $\lambda_1 > 0$.
4. The change in ambient density exponent from negative to positive, the shock strength, density ρ/ρ_1, and axial magnetic induction B_z/B_{z_1} decrease, but the pressure p/p_1 and fluid velocity u/u_1 increase, and the azimuthal magnetic induction B_θ/B_{θ_1} remains unchanged.

Author Contributions: G.N.: Proposed the problem, reviewed, edited and supervised. K.V.S.: Mathematical and numerical calculations, wrote the main manuscript text and prepared figures. All authors have read and agreed to the published version of the manuscript.

Funding: This research received no external funding.

Data Availability Statement: All the data related to this study are given in the manuscript.

Conflicts of Interest: The authors declare no conflict of interest.

References

1. Zel'Dovich, Y.B.; Raizer, Y.P. *Physics of Shock Waves and High-Temperature Hydrodynamic Phenomena*; Courier Corporation: North Chelmsford, MA, USA, 2002.
2. Hartmann, L. *Accretion Processes in Star Formation*; Cambridge University Press: Cambridge, UK, 2000; Volume 32.
3. Balick, B.; Frank, A. Shapes and shaping of planetary nebulae. *Annu. Rev. Astron. Astrophys.* **2002**, *40*, 439–486. [CrossRef]
4. Sedov, L. *Similarity and Dimensional Methods in Mechanics*; Academic Press: New York, NY, USA, 1959.
5. Lerche, I. Mathematical theory of one-dimensional isothermal blast waves in a magnetic field. *Aust. J. Phys.* **1979**, *32*, 491–502. [CrossRef]
6. Lerche, I. Mathematical theory of cylindrical isothermal blast waves in a magnetic field. *Aust. J. Phys.* **1981**, *34*, 279–302. [CrossRef]
7. Nath, G. Magnetogasdynamic shock wave generated by a moving piston in a rotational axisymmetric isothermal flow of perfect gas with variable density. *Adv. Space Res.* **2011**, *47*, 1463–1471. [CrossRef]
8. Vishwakarma, J.P.; Maurya, A.K.; Singh, K.K. Self-similar adiabatic flow headed by a magnetogasdynamic cylindrical shock wave in a rotating non-ideal gas. *Geophys. Astrophys. Fluid Dyn.* **2007**, *101*, 155–168. [CrossRef]
9. Mostert, W.; Wheatley, V.; Samtaney, R.; Pullin, D.I. Effects of magnetic fields on magnetohydrodynamic cylindrical and spherical richtmyer-meshkov instability. *Phys. Fluids* **2015**, *27*, 104102. [CrossRef]
10. Pai, S. *Cylindrical Shock Waves Produced by Instantaneous Energy Release in Magneto-Gas Dynamics*; Technical Report; University of Maryland, Institute for Fluid Dynamics and Applied Mathematics: College Park, MD, USA, 1958.
11. Sakurai, A. *Basic Developments in Fluid Dynamics*; Academic Press: New York, NY, USA, 1965; Volume 1.
12. Vishwakarma, J.P.; Patel, N. Cylindrical shock waves in a low conducting gas in presence of axial and azimuthal components of magnetic induction. *Res. Rev. J. Pure Appl. Phys.* **2013**, *1*, 23–34.
13. Vishwakarma, J.P.; Srivastava, R.K. Converging cylindrical detonation waves in a non-ideal gas with an azimuthal magnetic field. *Ganita* **2015**, *64*, 17–30.
14. Vishwakarma, J.P.; Nath, G.; Srivastava, R.K. Self-similar solution for cylindrical shock waves in a weakly conducting dusty gas. *Ain Shams Eng. J.* **2018**, *9*, 1717–1730. [CrossRef]
15. Bluman, G.W.; Cole, J.D. *Similarity Methods for Differential Equations*; Springer Science: New York, NY, USA, 1974.
16. Olver, P.J. *Application of Lie Group to Differential Equations*; Springer Science: New York, NY, USA, 1986.
17. Bluman, G.W.; Kumei, S. *Symmetries and Differential Equations*; Springer: New York, NY, USA, 1989.
18. Ovsiannikov, L.V. *Group Analysis of Differential Equation*; Academic Press: New York, NY, USA, 1982.
19. Hydon, P.E. *Symmetry Methods for Differential Equations: A Beginner's Guide*; Cambridge University Press: Cambridge, UK, 2000.
20. Ibragimov, N.H. *Elementory Lie Group Analysis and Differential Equations*; Wiley: Chichester, UK, 1999; Volume 2.
21. Golovin, S.V. Applications of the differential invariants of infinite dimensional groups in hydrodynamics. *Commun. Nonlinear Sci. Numer. Simul.* **2004**, *9*, 35–51. [CrossRef]
22. Golovin, S.V. Analytical description of stationary ideal MHD flows with constant total pressure. *Phys. Lett. A* **2010**, *374*, 901–905. [CrossRef]
23. Golovin, S.V. Natural curvilinear coordinates for ideal MHD equations. Non-stationary flows with constant total pressure. *Phys. Lett. A* **2011**, *375*, 283–290. [CrossRef]
24. Dorodnitsyn, V.A.; Kaptsov, E.I. Shallow water equations in Lagrangian coordinates: Symmetries, conservation laws and its preservation in difference models. *Commun. Nonlinear Sci. Numer. Simul.* **2020**, *89*, 105343. [CrossRef]
25. Dorodnitsyn, V.A.; Kaptsov, E.I.; Meleshko, S.V. Lie group symmetry analysis and invariant difference schemes of the two-dimensional shallow water equations in Lagrangian coordinates. *Commun. Nonlinear Sci. Numer. Simul.* **2023**, *119*, 107119. [CrossRef]
26. Logan, J.D.; Perez, J.d.J. Similarity solutions for reactive shock hydrodynamics. *SIAM J. Appl. Math.* **1980**, *39*, 512–527. [CrossRef]
27. Wang, X.-B.; Tian, S.-F.; Qin, C.-Y.; Zhang, T.-T. Lie symmetry analysis, analytical solutions, and conservation laws of the generalised whitham–broer–kaup–like equations. *Z. für Naturforschung A* **2017**, *72*, 269–279. [CrossRef]
28. Paliathanasis, A. Lie symmetries and similarity solutions for rotating shallow water. *Z. für Naturforschung A* **2019**, *74*, 869–877. [CrossRef]
29. Taylor, G.I. The formation of a blast wave by a very intense explosion I. theoretical discussion. *Proc. Math. Phys. Eng. Sci.* **1950**, *201*, 159–174.